

# Particle-in-Cell Simulations of the Slowing Down of Energetic Charged Particles in a Background Plasma

ALEXANDER CREELY

Princeton Plasma Physics Laboratory  
SULI Summer Intern

## Abstract

*The slowing down of a tenuous beam of energetic particles (EP) in background plasma has been well studied in situations where there is a magnetic field parallel to the particle motion and the beam's speed is less than that of the plasma's electrons, as is usually the case in Tokamaks. However, the influence of motion perpendicular to the magnetic field on this slowing is relatively unstudied, particularly when  $\rho_e/\lambda_D < 1$  and  $v_{ep}/v_{th,e} > 1$ . In order to predict the behavior of energetic particles in high-Beta machines such as a Field Reversed Configuration (FRC), one must investigate the effect of a perpendicular field on this slowing. To study this effect, simulations of a small number of energetic particles in background plasma were run using the Large Scale Plasma (LSP) Particle-in-Cell (PIC) code with no field, parallel field, and perpendicular magnetic field. Simulation parameters such as the energetic particle charge, the plasma density, the plasma temperature, and the simulation grid size were varied in order to achieve good energy conservation and the maximize accuracy of the particle slowing time. Slowing times for particles in a parallel field agreed with theoretical predictions to within a factor of 2. Results indicate that predictions for the slowing of energetic particles in Tokamaks will generally not apply to an FRC, and that the physics governing this phenomenon must be studied separately.*

## I. INTRODUCTION

With mankind's ever increasing hunger for more energy and the decreasing availability of fossil fuels, the search for alternative energy sources is becoming one of the largest challenges that humanity faces today. In light of its many advantages and theoretical backing, plasma fusion has emerged as one of the most hopeful prospects among the many types of alternative energy. While much attention has been given to studying and building Tokamaks and Stellarators, a number of other possible designs for a plasma fusion reactor are also in development. One such machine is known as the Field Reversed Configuration (FRC).

There are many differences between the physics governing a Tokamak and that governing an FRC, each of which must be studied closely before ap-

plying any theory of fusion in a Tokamak to fusion in an FRC. One such difference involves the magnetic field orientation in the region containing the plasma, particularly for the hottest particles, as the field is primarily parallel to particle motion in a Tokamak, but perpendicular to particle motion in an FRC. This difference is highly relevant to the slowing of energetic charged particles generated by fusion within the plasma.

A positively charged particle moving through a quasi-neutral background plasma will drag along with it a cloud of electrons through the Coulomb force and many Coulomb collisions.<sup>1,2</sup> The particle, however, will not be quite in the center of the cloud, which leads to a very slight electric field pointing opposite to the direction of motion. It is this electric field that leads to a drag force on the energetic particle and the subsequent slowing. However, a

<sup>1</sup>1. ITER Physics Expert Group on Energetic Particles, Heating and Current Drive, ITER Physics Basis Editors, and ITER EDA, Naka Joint Work Site, Mukouyama, Naka-machi, Naka-gun, Ibaraki-ken, Japan, "Chapter 5: Physics of energetic particles," Nuclear Fusion 39 (1999): 2474, accessed August 8, 2012, <http://iopscience.iop.org/0029-5515/39/12/305>.

<sup>2</sup>1. Nicholas A. Krall and Alvin W. Trivelpiece, Principles of Plasma Physics (New York: McGraw-Hill Book Company, 1973), 301

magnetic field can have a significant impact on the behavior of electrons in any plasma, particularly if the electron gyroradius is less than the Debye Length. This effect may also influence the manner in which the electron cloud moves and exerts its drag on the energetic particle, which in turn affects the rate at which the energetic particle loses kinetic energy.

As stated previously, a reasonable amount of time has already been dedicated to studying this slowing in a parallel magnetic field. In particular, Thomas Stix<sup>3</sup> made a theoretical prediction that energetic particles would slow to a thermal distribution with the characteristic slowing time  $\tau$  according to the following:

$$\tau = \frac{t_s}{3} \ln \left[ 1 + \left( \frac{W}{W_{crit}} \right)^{3/2} \right] \quad (1)$$

Where

$$W_{crit} = 14.8 kT_e \left[ \frac{A^{3/2}}{n_e} \sum \frac{n_j Z_j^2}{A_j} \right]^{2/3} \quad (2)$$

And

$$t_s = 6.27 * 10^8 \frac{A (kT_e)^{3/2}}{Z^2 n_e \ln \Lambda} \text{sec} \quad (3)$$

In which  $kT_e$  is the electron temperature in electron volts,  $W$  is the energetic particle energy in electron volts,  $A$  and  $A_j$  are the atomic mass of the energetic particles and background ions, respectively, in amu,  $n_e$  and  $n_j$  are the electron and background ion number density per  $\text{cm}^3$ ,  $Z$  and  $Z_j$  are the energetic particle and background ion charge in  $e$ , and  $\Lambda$  is the plasma parameter. While this formula fairly accurately describes the slowing of energetic particles in a parallel magnetic field,<sup>4</sup> the the physics governing the aforementioned mechanism behind the drag force calls into question its applicability in situations without a magnetic field, or with a magnetic field perpendicular to the particle motion.

This paper intends to investigate the difference in slowing times of energetic particles in background plasma with no magnetic field, with par-

allel magnetic field, and with perpendicular magnetic field. Simulations were run using Large Scale Plasma (LSP) code, which will be further described in the Computational Methods section. This section will also contain an explanation of the parameters and methods used when running LSP. The differences between the three magnetic field configurations were analyzed with a variety of simulation parameters in order to ensure that the results were repeatable. The Results and Discussion section will contain numeric and graphical representations of the outcomes of this study, and will discuss possible sources of error in the simulations. The paper will end by discussing the implications of the results in the Conclusions section.

## II. COMPUTATIONAL METHODS

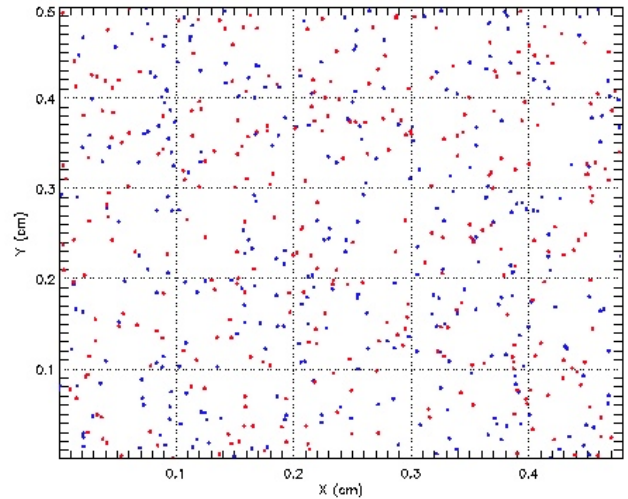


Figure 1: Particles in an LSP Simulation

As was mentioned above, this study was completed using LSP simulations. LSP is a Particle-in-Cell (PIC) code, which combines individual physical particles into larger super-particles, conserving mass, charge, etc., and then calculates the motion of these particles under the influence of external

<sup>3</sup>Thomas H. Stix, "Heating of Toroidal Plasmas by Neutral Injection," Plasma Physics 14 (1972): 375, accessed June 7, 2012, <http://iopscience.iop.org/0032-1028/14/4/002>.

<sup>4</sup>W. W. Heidbrink and G. J. Sadler, "The Behaviour of Fast Ions in Tokamak Experiments," Nuclear Fusion 34 (1994): 556, accessed August 8, 2012, <http://iopscience.iop.org/0029-5515/34/4/I07>.

<sup>5</sup>"LSP Suite: Particle-in-Cell (PIC) code for Large Scale Plasma Simulations," ATK Mission Systems, accessed August 8, 2012, last modified 2011, <http://www.mrcwdc.com/LSP/index.html>.

and particle-generated electric and magnetic fields.<sup>5</sup> This typically involves Coulomb scattering of the plasma particles, as well as their reaction to external fields and surfaces. LSP is able to run on either serial or parallel processors and has a large number of adjustable parameters in order to model a wide range of plasma systems.

Since the simulations in this study were only concerned with interactions within the plasma, rather than the interactions between the plasma and other objects, a fairly simple 2D rectangular geometry was employed. For simplicity, boundary conditions were made periodic (i.e. a particle leaving in the +x direction would reappear at the minimum x value, still moving in the +x direction) so that particles were contained within the system and particle-surface interactions could be ignored.

Simulations were all intended to run for 10 microseconds, but a number of the higher resolution trials ended up running for much shorter time spans due to computing time restraints. Some ran for as little as 200 nanoseconds. This time frame was selected as it was long enough to clearly recognize the decay trend, smoothing any temporary perturbations, but not so long as to require excessive computational time. The shorter runs had noticeably more fluctuation, but not enough to hinder further data analysis.

The following elements were the same in all of the simulations included in this study. The background plasma consisted of electrons, of mass 1 emu and charge -1 e, and deuterium ions, of mass 3675 emu and charge 1 e. The entire simulation space was seeded with a plasma of density  $10^{12}$  particles per  $\text{cm}^3$  and a temperature of 1 keV. The energetic particles in these simulations were protons with a mass of 1836 emu. The charge (Z) of these protons was altered in order to reduce the characteristic slowing time and thus reduce the runtime of the simulations. Typically the charge was 10 e. Consistent with the 14.7 MeV protons generated in Deuterium-Helium 3 fusion, in early simulations 14.7 MeV protons were injected along the  $y = 0$  line with no drift momentum. In later simulations, the energetic protons were injected along the  $y = 0$  line with thermal energy 1 MeV and a drift momentum of .17 Beta Gamma ( $\sim 13.7$  MeV) in the +y direction. The particles were injected for 0.01 ns with a current

of either 1A or 0.01 mA, depending on the trial.

The following parameters were varied slightly in order to attain the best energy conservation and the most accurate slowing times, as discussed below. The Courant Multiplier, defined as

$$C_o = \left| \frac{\Delta t * v}{\Delta x} \right| \leq 1 \quad (4)$$

governs the time step size  $\Delta t$  based on the speed of the particles in the simulation  $v$  and the cell size of the simulation grid  $\Delta x$ . In these simulations this multiplier was set at either 0.25 or 0.9, depending on the size of the particular trial. A number of preliminary trials revealed that 256 super-particles generated per simulation cell was a good balance between accuracy and runtime, but some trials were increased to 1024 particles per cell for increased accuracy. The number of x and y cells in the simulation grid was also adjusted in order to increase the accuracy of the simulation results. Earlier trials began with only one cell per centimeter, but later trials ended up moving to one cell per .01 centimeter, which was about half of the Debye length for those trials. Finally, the overall size of the simulation was adjusted in order to reduce the computational demands when the grid was set at finer resolutions, moving from 5 cm by 3 cm for earlier trials to .5 cm by .5 cm (about 21 Debye Lengths in each direction, as calculated later) for the finest resolution trials.

In order to obtain the desired results from this study, an external magnetic field was sometimes applied to the entire simulation space. While some trials had no magnetic field, those trials that did were always run in the presence of an 80 kG uniform magnetic field, which is consistent with another unique condition,  $\rho_e / \lambda_D < 1$ , in the FRC. In the case of the parallel magnetic field trials the field was aligned in the +y direction, and in the case of the perpendicular trials the field was aligned in the +z direction.

As was stated above, most simulations only ran for 10 microseconds or less. However, the slowing time for many of these trials was much longer, on the order of 10 milliseconds, as will become apparent later in this section. In order to account for this discrepancy, Mathematica was used to extrapolate the continued slowing of the energetic particles until such a time as they had reached a thermal distribution. Five points were taken from the energetic

particle kinetic energy data and fed into Mathematica, which then created an exponential fit curve, as seen below in Figure 2, consistent with Stix's assertion that the particles slow exponentially.<sup>6</sup> The point on this curve at which the energetic particles had cooled to the background plasma temperature of 1 keV was taken to be the characteristic slowing time described in Equation (1). Subsequently any references to the simulated energetic particle slowing time will refer to the time as determined by the method described here.

The fact that the majority of the simulations lost only on the order of 1% or less of their initial energy in the actual simulation time is obviously undesirable, but the trends observed in even these short simulation times seemed sufficient to estimate the total slowing time with some accuracy. Increasing the simulation time to greater than 10 microseconds was infeasible, as to run simulations with the fine resolution required for accurate results takes large amounts of time.

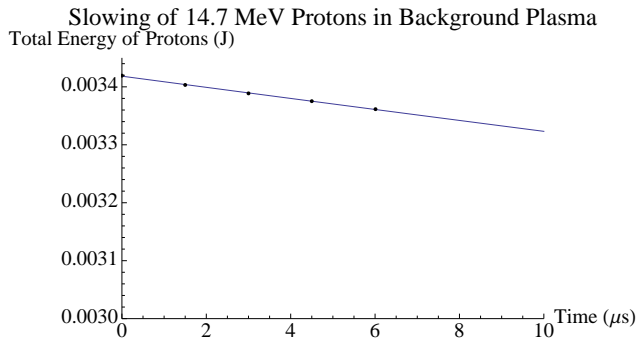


Figure 2: Exponential extrapolation of the slowing of energetic particles using Mathematica

The next section of this report will discuss the particular simulations and their results, but it should first be made clear that there were two parameters in particular which were used to judge the accuracy of the results of each trial: the overall energy conservation and the agreement between the parallel magnetic field run of a given set of simulations and the slowing time predicted by Equation (1).

Since LSP does not, and cannot, resolve cells or time steps to infinite precision, there is always some chance that information will be lost or distorted

during the calculation of particle motion, fields, or particle interaction. Moreover, if the cell does not resolve the Debye Length, then the plasma particles tend to grow in energy until their energy is large enough to make the Debye Length match the cell size. Since the slowing process is caused by Debye Length-scale electric fields, it seems that resolving the Debye Length would be necessary. LSP has some measures to combat these inaccuracies, but they are not always effective, and as such, energy conservation is not always perfect. Even if the cell does resolve the Debye Length, perfect energy conservation is by no means assured. For this reason, one must keep a close eye on the total energy conservation of the system in any given simulation. If the energy growth or decline is large enough, it may very well distort the slowing time of the energetic particles, as the temperature of the background plasma would no longer be constant and the energetic particles themselves may experience artificial heating as well. In the later discussion of individual trials, energy conservation will always be examined to ensure that it fits within acceptable ranges.

In addition to looking at energy conservation, the trials below will also be evaluated based on their agreement with the slowing time predicted by Stix in Equation (1). Since this formula has both theoretical and experimental backing, the validity of the parallel magnetic field simulation results created here is highly dependent on the agreement between the two. Some differences are to be expected, as the code is by no means a perfect replica of reality, but results should at least agree in order of magnitude, otherwise even qualitative results are probably untrustworthy. Should the results agree with the Stix prediction to a much greater degree then it may be reasonable to place trust in both the qualitative and quantitative results from these simulations. For this reason, the agreement with the Stix predictions was the second main criteria by which the accuracy of the simulation sets were judged.

Specifically, the simulations in this study will employ the following parameters in Equation (1):  $W = 14.7$  MeV,  $kT_e = 1$  keV,  $A = 1.008$ ,  $n_e = 10^{12}$ ,  $n_j = 10^{12}$ ,  $Z_j = 1$ ,  $A_j = 2.014$  (where subscript  $j$  refers only to deuterium),  $Z = 10$ , and  $\ln \lambda = 20$ . If one cal-

<sup>6</sup>Stix, 375.

culates  $\tau$  from Equation (1) using these parameters, one finds that  $\tau = 36.77$  ms for  $Z = 10$ . These values will be compared to the simulation results in the next section.

Using this computational setup, the following results were obtained.

### III. RESULTS AND DISCUSSION

The results of two separate simulation setups will be presented in this section in order to show the differences in the overall results in less than ideal computational situations. Each set includes simulations with no field, with parallel field, and with perpendicular magnetic field. All results are summarized below in Table 1.

The first set of simulations, Set 1, was conducted with a slightly larger plasma and a rougher grid resolution, one that did not resolve the Debye Length. As stated above, this simulation contained an electron and deuterium plasma at 1 keV and  $10^{12}$  particles per  $\text{cm}^3$ . Due to the rougher grid resolution, to be explored below, these simulations were run at 1024 particles per cell and a Courant Multiplier of 0.25. Protons at 14.7 MeV with  $Z = 10$  were injected with a thermal distribution along the  $y = 0$  line at 1 amp.

The simulation expanded 5 cm in the  $x$  direction and 3 cm in the  $y$  direction, and had 90 cells in the  $x$  direction and 3 cells in the  $y$  direction. This set of simulations did not resolve the Debye Length, defined as

$$\lambda_D = \left(\frac{kT}{4\pi ne^2}\right)^{1/2} \quad (5)$$

which can be calculated as 0.0235 cm in a 1 keV plasma with a density of  $10^{12}$  per  $\text{cm}^3$ . The next set of simulations, to be presented below, however, did resolve the Debye Length, to which their greater accuracy may be attributed.

The  $x$  coordinate was resolved much more finely than the  $y$  coordinate because the energetic particles were primarily moving in the  $+y$  direction, which meant that they remained in the same  $x$  cell for far longer than they remained in the same  $y$  cell. Additional  $x$  cells enabled the use of additional processors, as per the LSP requirement that each processor contain at least 3 cells in the split

direction, and splitting in the  $x$  direction meant that energetic particles stayed, for the most part, in the region of the simulation governed by one processor, rather than quickly moving between processor regions. This splitting, which reduced energetic particle transfers between processor regions, greatly increased the speed and energy conservation of the simulations.

These particular simulations were run on 30 processors, split in the  $x$  direction, and took 192 hours to run for approximately 8 microseconds.

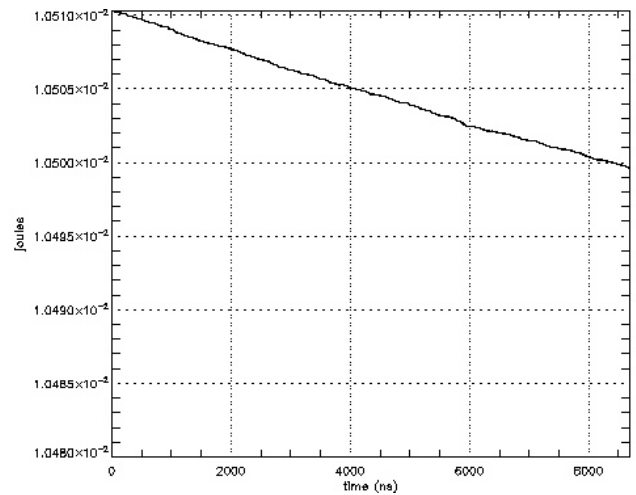


Figure 3: Total Energy of Set 1 Parallel Magnetic Field LSP System

As was mentioned above, one must first consider the energy conservation of these trials in order to determine their validity. Beginning with the parallel magnetic field trial, the system started with a total of 0.0105014 J of energy and after 8.69 microseconds had 0.0104996 J of energy, for a loss of  $1.08 \times 10^{-5}$  J or 0.102% of the initial total energy. Similarly the trial without magnetic field began with 0.0106281 J of energy and ended with 0.0106217 J after 6.01 microseconds, for a loss of  $6.4 \times 10^{-6}$  J or 0.060% of the initial energy. The trial with perpendicular magnetic field began with 0.0106067 J of total energy and ended with 0.0105983 J after 7.47 microseconds, for a loss of  $8.4 \times 10^{-6}$  J or 0.079% of the initial total energy. These energy losses are small compared to the change in the energetic particle energy, which speaks to the accuracy of the trials, but still of the same order of magnitude, which still leaves some

room for doubt. The raw energy data for the parallel magnetic field run can be seen in Figure 3.

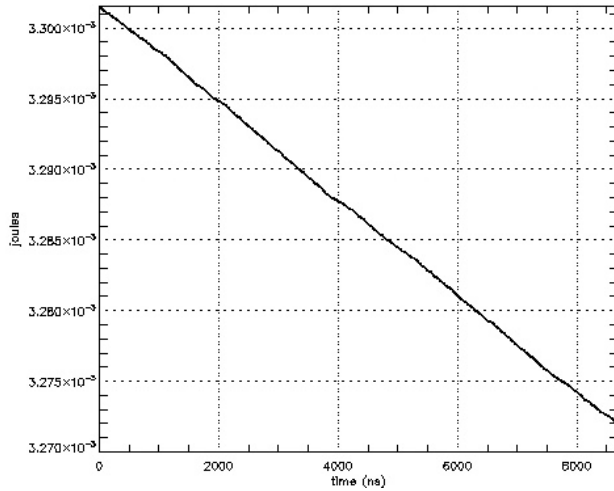


Figure 4: Total Proton Energy of Set 1 Parallel Magnetic Field Trial

In terms of the proton slowing, this set of trials did not agree quite as closely with the Stix prediction as might have been hoped. However, qualitative comparisons between the three magnetic field configurations may still be made. The parallel magnetic field trial protons began with a total of 0.00330155 J of kinetic energy and ended with 0.00327211 J after 8.69 microseconds, losing 0.892% of the initial kinetic energy. An exponential extrapolation with Mathematica gives a slowing time of 9.26 ms. The protons with no magnetic field began with a total of 0.00341933 J of kinetic energy and ended with 0.00336146 J after 6.01 microseconds, losing 1.692% of the initial kinetic energy. An exponential extrapolation gives a slowing time of 3.40 ms. Finally, the protons in the perpendicular magnetic field began with 0.00339760 J of energy, and ended with 0.00339415 J after 7.47 microseconds, for a loss of 0.101%. This gives a slowing time of 71.41 ms. Raw data for the parallel magnetic field trial can be seen in Figure 4.

The second set of simulations, Set 2, was run on a smaller plasma with a finer grid resolution. The background plasma was the same as the first run, consisting of 1 keV and  $10^{12}$  particles per  $\text{cm}^3$  electrons and deuterium. Due to the finer grid resolution, these simulations were run with 256 particles

per cell and at a Courant Multiplier of 0.9. The energetic particles were injected along the  $y = 0$  line with thermal energy  $1 \times 10^6$  eV and a drift momentum of 0.17 Beta Gamma ( $\sim 13.7$  MeV) in the +y direction for .01 ns at .01 mA. The protons in Set 2 were also of charge  $Z = 10$ .

These grid in these simulations expanded .5 cm in the x direction and .5 cm in the y direction. There were 100 x cells and 50 y cells so that unlike the previous set of simulations, these resolved the Debye length (of 0.0235 cm as before) in both the x and the y directions. The increased x cells were again intended to allow additional processors as previously explained.

These simulations were run on 32 processors, split in the x direction, and took 100 hours to run for approximately 200 nanoseconds.

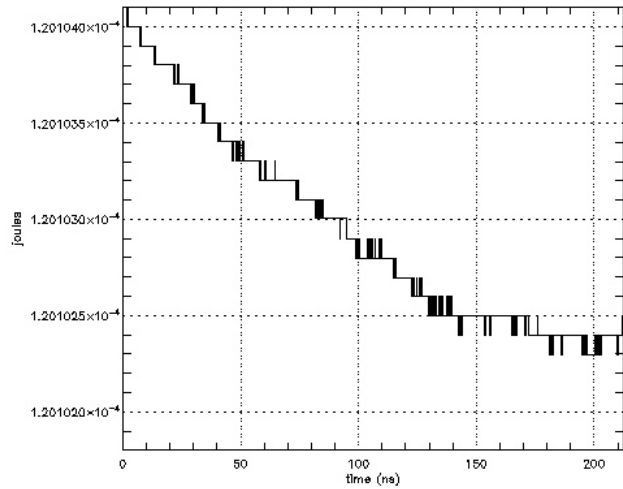


Figure 5: Total Energy of Set 2 Parallel Magnetic Field LSP System

Looking first at energy conservation of the Set 2 simulations, the parallel magnetic field system started with a total of  $1.20104 \times 10^{-4}$  J of energy and after 0.212 microseconds had  $1.20102 \times 10^{-4}$  J of energy, for a loss of 0.00166% of the initial total energy. The trial without magnetic field also began with  $1.20104 \times 10^{-4}$  J of energy and ended with  $1.20102 \times 10^{-4}$  J after 0.241 microseconds, for a loss of 0.00166% of the initial energy. The Set 2 trial with perpendicular magnetic field began with  $1.20105 \times 10^{-4}$  J of total energy and ended with  $1.20104 \times 10^{-4}$  J after 0.168 microseconds, for a loss

Set	Magnetic Field	Runtime ( $\mu$ s)	Energy Conservation (%)	Proton Energy (%)	Slowing Time (ms)
1	Parallel	8.69	0.102	0.892	9.26
1	None	6.01	0.060	1.692	3.40
1	Perpendicular	7.47	0.079	0.101	71.41
2	Parallel	0.212	0.00166	0.015	14.06
2	None	0.241	0.00166	0.014	16.19
2	Perpendicular	0.197	0.00083	0.005	39.10

Table 1: Energy Conservation and Slowing Data from Simulation Sets 1 and 2

of 0.00083% of the initial total energy. The parallel field trial total energy raw data can be seen in Figure 5. The energy conservation of Set 2 is far superior to that of Set 1, as the percentage energy loss is orders of magnitude smaller than the percentage slowing of the protons. Some of this may be attributed to the shorter runtimes, but it still speaks to the accuracy of the simulations.

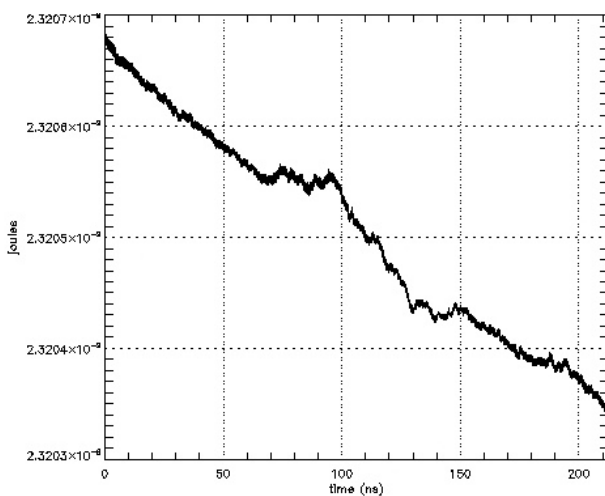


Figure 6: Total Proton Energy of Set 2 Parallel Magnetic Field Trial

The Set 2 parallel magnetic field trial protons began with a total of  $2.32068 \times 10^{-9}$  J of kinetic energy and ended with  $2.32034 \times 10^{-9}$  J after 0.212 microseconds, losing 0.0146% of the initial kinetic energy. An exponential extrapolation with Mathematica gives a slowing time of 14.06 ms. The protons with no magnetic field began with a total of  $2.37257 \times 10^{-9}$  J of kinetic energy and ended with  $2.37222 \times 10^{-9}$  J after 0.241 microseconds, losing 0.0147% of the

initial kinetic energy. An exponential extrapolation gives a slowing time of 16.19 ms. Finally, the protons in the perpendicular magnetic field began with  $2.35216 \times 10^{-9}$  J of energy, and ended with  $2.35204 \times 10^{-9}$  J after 0.168 microseconds, for a loss of 0.0051%. This gives a slowing time of 39.10 ms. The parallel field proton slowing data can be seen in Figure 6.

In analyzing the data, the largest cause for concern is the marked disagreement between the theoretical prediction and the computational results for the slowing time of energetic particles in a parallel magnetic field. As stated above, Equation (1) predicts that with  $Z = 10$ , the slowing time should be approximately 36.77 ms. However, in parallel magnetic field Set 1 parameters resulted in a slowing time of 9.26 ms and Set 2 parameters resulted in a slowing time of 14.06 ms. Even the higher resolution simulations are off by a factor of approximately 2, which is certainly unsettling. The sources of error that may have led to this discrepancy are discussed below. However, the fact that the computed slowing times are still on the same order of magnitude as the predictions, and considering that there are plausible explanations for the discrepancy between theory and computation, it still seems reasonable to analyze the results qualitatively and compare the slowing times of the energetic particles in the three magnetic field cases.

Even qualitatively, however, the results are not entirely consistent. In Set 1, the trial without magnetic field has the shortest slowing time, followed by the parallel magnetic field case, and then the perpendicular magnetic field case had a time that was much longer. In Set 2, however, it was the parallel magnetic field case that had the shortest slowing

time, followed by the trial without magnetic field, and finally the perpendicular field case. In addition to the sources of error discussed below, the most plausible explanation for this difference is the fact that Set 1 does not resolve the Debye Length while Set 2 does. Additional simulation sets not included in this paper reveal that sets that do not resolve the Debye Length show the runs with no magnetic field having the shortest slowing time, while sets that do show the parallel field runs having the shortest slowing time. All runs, regardless of Debye Length resolution, however, reveal that energetic particles in a perpendicular magnetic field take the longest to slow down. Despite the problems with the consistency of other runs, trends in this study seem to speak to the fact that the slowing process is fundamentally different in situations with different magnetic field orientations, and that estimations for one situation are of questionable validity in any other. In addition, the distinct differences between the trials that do and don't resolve the Debye Length suggest that this parameter is paramount in importance in LSP simulations and that future simulations intending to study phenomenon governed by Debye Length-scale physics must certainly resolve this length in order to ensure the validity of the results.

As the only moderate agreement with theoretical predictions indicates, this study still contains a number of possible sources of error. First and foremost, any simulation inherently relies on an artificial environment in which to complete the calculations of forces and motion, which allows for the possibility of computational error at the level of individual calculations. In addition, the LSP code, while quite good, is not a perfect replica of reality. The grouping of individual particles into super-particles may very well have some unanticipated consequences, which may be left uncorrected by LSP or any PIC code. The particular parameters in this study, limited as they were by computational power and time, may also have contributed to inaccuracies in the results. Furthermore, despite evidence in earlier simulations not included in this paper that there is only negligible difference between the results of

2D and 3D simulations, the fact that all of these trials were in two dimensions may still have had some influence on the results. Finally, since the final slowing times were calculated by exponential fit rather than by direct simulation, the relatively short simulation time as compared to the overall slowing time may have led to problems with the accuracy of the exponential fit. While these sources may have all contributed in some way or another to errors in this study, the order of magnitude agreement with theoretical predictions is evidence as to the general qualitative validity of these results.

#### IV. CONCLUSION

This study investigated the impact of magnetic fields on the slowing of energetic particles in a background plasma using LSP code. In particular, the difference in slowing times in no magnetic field, in parallel field, and in perpendicular field were of interest for conditions that are found in a typical plasma in an FRC. While disagreements between theoretical predictions and the simulation results call into question the validity of any quantitative results from this study, the study was useful qualitatively in both understanding LSP code and the significance of the impact of magnetic fields on energetic particle slowing. This study found that in order to legitimately study any phenomenon governed by Debye Length-scale physics using LSP, one must make sure to resolve this length with the simulation grid. In terms of the physics, this study found that the presence and orientation of a magnetic field most certainly have an effect on the slowing time of energetic particles in a background plasma. More tentatively, this study can conclude that a perpendicular magnetic field significantly increases the slowing time of energetic particles, but can make no definite claims as to the effect of a parallel magnetic field. These results suggest that predictions for particle slowing in Tokamaks are invalid in an FRC and justify additional research into the physics governing the slowing of energetic charged particles in a background plasma with magnetic field.

## V. ACKNOWLEDGEMENTS

I would first like to thank Professor Sam Cohen of the Princeton Plasma Physics Laboratory, who was my mentor in the Summer of 2012 and without which this research would never have happened. He taught me much of what I needed to know to complete this research and contributed greatly to the analysis of the results, the content of the paper, and its styling. The results themselves were primarily intended to further the research goals of Professor Cohen's work. In addition, I would like to thank Dale Welch of Voss Scientific, who gave me a lot of help with the LSP code and made a number of suggestions as to how to improve the overall accuracy of the results. Finally, I would like to thank the Summer Undergraduate Laboratory Internship program funded by the DOE Office of Workforce Development for Teachers and Students, which funded the internship during which I completed this research. Without their backing I would not have had the opportunity to complete this study.

VI. APPENDIX: SET 2 Z = 10 PARALLEL MAGNETIC FIELD LSP FILE

```

;GLSP version 6.91 : GLSP_120201
;(08/09/2012 15:23:47)
;GLSP comments --BEGIN--
;GLSP comments --END--
;GLSP compiler flags --BEGIN--
; CAR_X_Y CHARGE_DENSITY COLLISIONAL_PLASMA DOUBLE_PRECISION
; EXTENDED_PARTICLES EXTERNAL_BFIELDS=1 IONIZATION_ON MAX_CHARGE_STATE=7
; MAX_SPECIES=5 MULTI_PROCESS MUTABLE_SPECIES=1 NUMBER_DENSITIES
; PRIMARY_SPECIES=1 SCATTERING_ON
;GLSP compiler flags --END--
;GLSP metric: 0 dimensions: xy
[Control]
;Time-advance
courant_multiplier 0.9
time_limit_ns 1.0E+04
;(Diagnostic Output) Dump Intervals
probe_interval 1
;
[Grid]
;
grid1 ; grid 1
xmin          0.0
xmax          0.5
x-cells       100
;
ymin          0.0
ymax          0.5
y-cells       50
;
;
[Regions]
;
region1 ; region1
;
grid 1
xmin 0.0
xmax 0.5
ymin 0.0
ymax 0.5
number_of_domains 32
split_direction XSPLIT
number_of_cells AUTO
;
;
[Boundaries]
;
periodic ; theta

```

```

from 0 0 0
to 0.5 0.5 1
normal Y
;
periodic ; sides
from 0 0 0
to 0.5 0.5 1
normal X
;
[ExternalFields]
external1 ; magnetic
type CONSTANT
field B Y 8.0E+04
temporal_function 7
;
;
[Particle Species]
species1 ; electron
charge -1.0
mass 1.0
migrant_species_flag off
implicit_species_flag off
particle_motion_flag on
particle_forces_option PRIMARY
transverse_weighting_flag on
particle_kinematics_option STANDARD
scattering_flag on
selection_ratio 1.0
;
species2 ; deuterium
charge 1.0
mass 3.675E+03
atomic_number 1
migrant_species_flag off
implicit_species_flag off
particle_motion_flag on
particle_forces_option PRIMARY
transverse_weighting_flag on
particle_kinematics_option STANDARD
scattering_flag on
selection_ratio 1.0
;
species3 ; proton
charge 10
mass 1.836E+03
atomic_number 1
migrant_species_flag off
implicit_species_flag off

```

```

particle_motion_flag on
particle_forces_option PRIMARY
transverse_weighting_flag on
particle_kinematics_option STANDARD
scattering_flag on
selection_ratio 1.0
;
;
[Particle Creation]
;
plasma ; initial electrons
from 0 0.0 0.0
to 0.5 0.5 0.0
species 1
movie_tag 1
unbound off
discrete_numbers 16 16 1
random off
multiple_number 1
cloud_radius 0.0
density_function 2
momentum_function 0
reference_point 0.0 0.0 0.0
density_flags 0 0 0
momentum_flags 0 0 0
drift_velocity 0.0 0 0
rotation off
thermal_energy 1.0E+03
random_energy_function 0
spatial_function 0
movie_fraction 0.1
;
plasma ; initial ions
from 0 0.0 0.0
to 0.5 0.5 0.0
species 2
movie_tag 2
unbound off
discrete_numbers 16 16 1
random off
multiple_number 1
cloud_radius 0.0
density_function 2
momentum_function 0
reference_point 0.0 0.0 0.0
density_flags 0 0 0
momentum_flags 0 0 0
drift_velocity 0.0 0 0

```

```

rotation off
thermal_energy 1.0E+03
random_energy_function 0
spatial_function 0
movie_fraction 0.5
;
injection
from 0 0.0 0.0
to 0.5 0.0 0.0
normal Y
interval 1
species 3
movie_tag 3
discrete_numbers 1 1 1
random off
temporal_function 5
spatial_function 6
radius_function 0
drift_momentum 0.0 0.17 0.0
spatial_momentum_function 0
temporal_momentum_function 0
centroid1_function 0
centroid2_function 0
reference_point 0.0 0.0 0.0
spatial_flags 0 0 0
deflection1_angle 0.0
deflection2_angle 0.0
convergence off
rotation off
distribution_type GAUSSIAN
thermal_energy 1.0E+06
random_energy_function 0
movie_fraction 1
;
[Functions]
function1 ; Magnetic Field
type 1
coefficients 80000 end
;
function2 ; Initial Density
type 1
coefficients 1e12 end
;
function5 ; Injection Pulse
type 3
coefficients 0.00001 0.01 end
;
function6 ; Proton Injection Spatial

```

```
type 1
coefficients 100 end
;
function7 ; constant 1
type 1
coefficients 1 end
;
;
[Probes]
;
probe1 ; number1
global number species 1
;
probe2 ; number2
global number species 2
;
probe3 ;
energy total_energy
;
probe4 ;
energy particle_energy
;
probe5 ; ketot1
global ketot species 1
;
probe6 ; ketot2
global ketot species 2
;
probe7 ;
energy net_energy
;
probe8 ; ocmax1
global ocmax species 1
;
probe9 ; opmax1
global opmax species 1
;
probe10 ; ketot3
global ketot species 3
;
probe11 ; number3
global number species 3
;
```